ELSEVIER

1 July 1996

PHYSICS LETTERS A

Physics Letters A 217 (1996) 59–64

Long-range effects on optical absorption in quasiperiodic lattices

Francisco Domínguez-Adame [1]

Departamento de Física de Materiales, Facultad de Físicas, Universidad Complutense, E-28040 Madrid, Spain

Received 23 March 1996; accepted for publication 2 April 1996
Communicated by V.M. Agranovich

Abstract

We consider exciton optical absorption in quasiperiodic lattices, focusing our attention on the Fibonacci case as a typical example. The absorption spectrum is evaluated by solving numerically the equation of motion of the Frenkel-exciton problem on the lattice, in which on-site energies take on two values according to the Fibonacci sequence. We find that the quasiperiodic order causes the occurrence of well-defined characteristic features in the absorption spectra. We also develop an analytical method that relates satellite lines with the Fourier pattern of the lattice. Our predictions can be used to determine experimentally the long-range quasiperiodic order from optical measurements.

PACS: 71.35.+z; 36.20.Kd; 61.44.+p

1. Introduction

Linear lattices described by means of the binary Fibonacci sequence have been regarded as one-dimensional (1D) quasicrystals and, consequently, they have been the subject of intensive theoretical studies. These systems lack translational symmetry but, unlike disordered lattices, display long-range order. The corresponding electronic states present rather unusual properties like fractal energy spectra and self-similar wave functions. From the experimental viewpoint, several electronic properties of solids can be inferred from optical characterization techniques like optical absorption, photoluminescence and fluorescence after pulse excitation. Then, a complete understanding of the interplay between the electronic properties and the underlying quasiperiodic order requires a detailed analysis of optical processes. This reason has motivated various works dealing with optical properties of Fibonacci systems, mainly devoted to Fibonacci semiconductor superlattices [1–4].

In previous works we have focused our attention on excitons in Fibonacci lattices [5,6]. In particular, we have numerically evaluated optical absorption spectra due to Frenkel excitons in self-similar aperiodic lattices (Fibonacci and Thue–Morse) [5]. We found several characteristic lines specific of each aperiodic system that are not present in periodic or random Frenkel lattices, thus being an adequate way for determining the particular structural order of the system from experiments. When the two kinds of optical centers composing the aperiodic lattice are very different, the origin of all the absorption lines can be successfully assigned by considering the aperiodic lattices as composed of two-center blocks, in the same spirit as the renormalization group concepts

[1] E-mail: adame@eucmos.sim.ucm.es.

PII S0375-9601(96)00314-3

developed in the last few years [7,8]. This approach neglects the long-range order present in the lattice and only takes into account the short-range interaction between nearest-neighbor optical centers. These results lead, in a natural way, to the question whether long-range quasiperiodic order can also be characterized by means of optical absorption spectra. It is clear that we must search for specific lines due to the long-range order in the opposite limit, namely when the two kinds of optical centers are of similar nature. We will show below that this is indeed the case.

In this work we investigate optical absorption due to Frenkel excitons in 1D binary systems arranged according to the Fibonacci sequence. We make use of a general treatment which allows us to study the dynamics of Frenkel excitons in these lattices, solve the microscopic equations of motion and find the optical absorption spectrum. The main conclusions of this paper are twofold. First, we show that Frenkel excitons in Fibonacci lattices with similar optical centers lead to absorption lines specific of this kind of ordering and, consequently, not present in periodic or disordered lattices. Second, and most important, by means of an analytical approach we are able to explain the origin of these characteristic lines, which are related to the Fourier transform of the lattice. Thus we successfully relate an optical property (optical spectrum) with a structural one (topology of the lattice).

2. Physical model and theory

We consider a system of N optically active, two-level centers, occupying positions $\boldsymbol{r}_n$ on a 1D regular lattice with spacing unity. Therefore, the effective Frenkel Hamiltonian describing this system can be written (we use units such that $\hbar = 1$)

$$\mathscr{H} = \sum_n V_n a_n^\dagger a_n + \sum_{l \neq n} J_{nl} a_n^\dagger a_l . \tag{1}$$

Here $a_n^\dagger$ and a_n creates and annihilates an electronic excitation of energy V_n at site n, respectively. J_{nl} $(n \neq l)$ is the intersite interaction of dipole origin between the centers n and l, assumed to be of the form $J_{nl} = -J\,|\,\boldsymbol{r}_n - \boldsymbol{r}_l\,|^{-3}$, where J is the coupling between the nearest-neighbor centers. Since J_{nl} is a rapidly decreasing function of the distance between the centers, we will omit interactions beyond nearest neighbors.

In this work we will be concerned with the Frenkel exciton dynamics in systems presenting a quasiperiodic distribution of optical centers. The Fibonacci lattice is the archetypical example of deterministic and quasiperiodically ordered structure. Any arbitrary Fibonacci system presents two kinds of building blocks. In our case, we choose those blocks as individual two-level centers with on-site energies V_A and V_B. The Fibonacci arrangement can be generated by the substitution rule $A \rightarrow AB$, $B \rightarrow A$. In this way, finite and self-similar quasiperiodic lattices are obtained by n successive applications of the substitution rule. The nth generation lattice will have $N = F_n$ elements, where F_n denotes a Fibonacci number. Such numbers are generated from the recurrence law $F_n = F_{n-1} + F_{n-2}$ starting with $F_0 = F_1 = 1$; as n increases the ratio F_{n-1}/F_n converges toward $\tau = \frac{1}{2}(\sqrt{5} - 1) = 0.618\ldots$, an irrational number which is known as the inverse golden mean. Therefore, lattice sites are arranged according to the Fibonacci sequence $V_A V_B V_A V_A V_B V_A V_B V_A \ldots$, where the fraction of B-centers is $c \sim 1 - \tau$.

Having presented our model we now briefly describe the method we have used to calculate the absorption spectra. The line shape $I(E)$ of an optical-absorption process in which a single exciton is created in a lattice with N sites can be obtained as follows [9]. Let us consider the total dipole moment operator $\mathscr{D} = \sum_n (a_n^\dagger + a_n)$, where the dipole moment of each center is taken to be unity. Here we restrict ourselves to the case of systems whose length is much smaller than the optical wavelength. Denoting by $|k\rangle$ and E_k the eigenvectors and eigenvalues of the Hamiltonian $\mathscr{H}$, respectively, the absorption line-shape is given by

$$I(E) = \frac{1}{N} \sum_k |\langle k | \mathscr{D} | \mathrm{vac} \rangle|^2 \delta(E - E_k), \tag{2}$$

where $|\mathrm{vac}\rangle$ denotes the exciton vacuum. In practice one considers a broadened δ-function to take into account the instrumental resolution function. Therefore we will replace the δ-function by a Lorentzian function of half-width α, hereafter denoted by δ_α.

A reliable method for determining $I(E)$ numerically involves the consideration of the correlation functions [9]

$$G_n(t) = \sum_l \langle \mathrm{vac} \mid a_n(t)\, a_l^\dagger \mid \mathrm{vac} \rangle, \tag{3}$$

where $a_n(t) = \exp(\mathrm{i}\mathscr{H}t) a_n \exp(-\mathrm{i}\mathscr{H}t)$ is the annihilation operator in the Heisenberg representation. The function $G_n(t)$ obeys the equation of motion

$$\mathrm{i}\frac{\mathrm{d}}{\mathrm{d}t} G_n(t) = \sum_l H_{nl} G_l(t), \tag{4}$$

with the initial condition $G_n(0) = 1$. The diagonal elements of the tridiagonal matrix H_{nl} are V_n, whereas the off-diagonal elements are simply given by $-J$. The microscopic equation of motion is a discrete Schrödinger-like equation on a lattice and standard numerical techniques may be applied to obtain the solution. Once these equations of motion are solved, the line shape is found from the following expression,

$$I(E) = -\frac{2}{\pi N} \int_0^\infty \mathrm{d}t\, \mathrm{e}^{-\alpha t} \sin(Et)\, \mathrm{Im}\Big(\sum_n G_n(t) \Big), \tag{5}$$

where the factor $\exp(-\alpha t)$ takes into account the broadening due to the instrumental resolution function of half-width α.

3. Numerical results

We have solved numerically the equation of motion (4) using an implicit (Crank–Nicholson) integration scheme [10]. In the remainder of the paper, energy will be measured in units of J whereas time will be expressed in units of J^{-1}. The energy and time scales can deduced from the experiment since the exciton bandwidth is $4J$. Fibonacci lattices are generated using the inflation rules discussed above. In order to minimize end effects, spatial periodic boundary conditions are introduced in all cases. We have checked that the position and the strength of all lines of the spectra are independent of the system size. Hereafter we will take $N = F_{12} = 233$ as a representative value. We have set $V_A = 4.0$, $V_B = 4.8$ and $J = 1$ as typical values corresponding to centers with similar characteristics. The width of the instrumental resolution was $\alpha = 0.15$. The maximum integration time and the integration time step were 50 and 10^{-3}, respectively. Smaller time steps lead essentially to the same results.

In the pure A lattice the spectrum is a single Lorentzian line centered at $E = V_A - 2J = 2.0$, with our choice of parameters. When B-centers are introduced according to the Fibonacci rules, a shift of the position of the main line towards higher energies is observed. This shift is also observed in the case of random lattices [11,12]. The main line is now located around $E = 2.30$, as shown in Fig. 1. Besides this main absorption line, two satellite lines can be also observed in the high-energy part of the spectrum, centered at energies $E^{(1)} = 5.92$ and $E^{(2)} = 4.03$. According to the renormalization group techniques developed in Ref. [5], none of these satellites can be explained within the so-called two-center approach. Thus we are led to the conclusion that they are due to long-range effects of the quasiperiodic ordering of the lattice. This will be more evident after performing the analytical treatment.

4. Analytical results

In this section we develop a theoretical approach to explain the shift of the main line and the occurrence of well-defined satellite lines in the high-energy region when B-centers are introduced quasiperiodically in the lattice. To this end we rewrite the system Hamiltonian $\mathscr{H} = \mathscr{H}_A + \mathscr{H}_{AB}$, where

$$\mathscr{H}_A = V_A \sum_n a_n^\dagger a_n - J \sum_n \left(a_n^\dagger a_{n+1} + a_{n+1}^\dagger a_n \right), \tag{6a}$$

$$\mathscr{H}_{AB} = \sum_n (V_n - V_A)\, a_n^\dagger a_n. \tag{6b}$$

Here $\mathscr{H}_A$ is the Hamiltonian corresponding to the pure A lattice.

As a first step we consider the pure A lattice whose Hamiltonian is $\mathscr{H}_A$. This Hamiltonian with periodic boundary conditions can be exactly diagonalized, yielding the eigenvectors

$$\mid k \rangle = \left(\frac{1}{N} \right)^{1/2} \sum_n \exp(2\pi \mathrm{i} nk/N)\, a_n^\dagger \mid \mathrm{vac} \rangle, \tag{7a}$$

with $k = 0, \ldots, N-1$. The corresponding eigenvalues read

$$E_k = V_A - 2J\cos(2\pi k/N). \tag{7b}$$

Therefore, the dipole moment matrix elements within this approximation satisfy the relation $\langle k|\mathscr{D}|\mathrm{vac}\rangle = \delta_{k0}$. Consequently, one obtains that $I(E) = (1/N)\delta_\alpha(E - E_0)$. This result shows that the pure A lattice presents a single Lorentzian absorption line centered at $E_0 = V_A - 2J$, as we have mentioned above.

To develop an approach that can explain the results in Fibonacci systems one must explicitly consider the effects of the topology through the term $\mathscr{H}_{AB}$. To carry out such an approximation we have used the nondegenerate perturbation theory. Let $|k^{(AB)}\rangle$ be the perturbed eigenvector describing the exciton state when the influence of the term $\mathscr{H}_{AB}$ is taken into account. To evaluate the perturbed dipole moment matrix element, we expand $|k^{(AB)}\rangle$ in the basis of the unperturbed eigenvectors $|k\rangle$ given in (7a)

$$|k^{(AB)}\rangle = |k\rangle + \sum_{l\neq k} \frac{\langle l|\mathscr{H}_{AB}|k\rangle}{E_k - E_l}|l\rangle, \tag{8a}$$

whereas the perturbed eigenvalues are given by

$$E_k^{(AB)} = E_k + \langle k|\mathscr{H}_{AB}|k\rangle = E_0^{(AB)} + 4J\sin^2(\pi k/N), \tag{8b}$$

where $E_0^{(AB)} = cV_B + (1-c)V_A - 2J$. Notice that $\mathscr{H}_{AB}$ shifts all levels by the same amount. This shift is given by $\langle k|\mathscr{H}_{AB}|k\rangle = c(V_B - V_A)$ for all k. With the chosen parameters this amounts to 0.30, in perfect agreement with our numerical results shown in Fig. 1.

Inserting (8) in (2) one finally obtains

$$I(E) = \frac{1}{N}\delta_\alpha\left(E - E_0^{(AB)}\right) + \frac{1}{N}\sum_{k=1}^{N-1}|F(k)|^2\delta_\alpha\left(E - E_k^{(AB)}\right), \tag{9}$$

where for brevity we have defined

$$F(k) \equiv \frac{\langle 0|\mathscr{H}_{AB}|k\rangle}{4J\sin^2(\pi k/N)}. \tag{10}$$

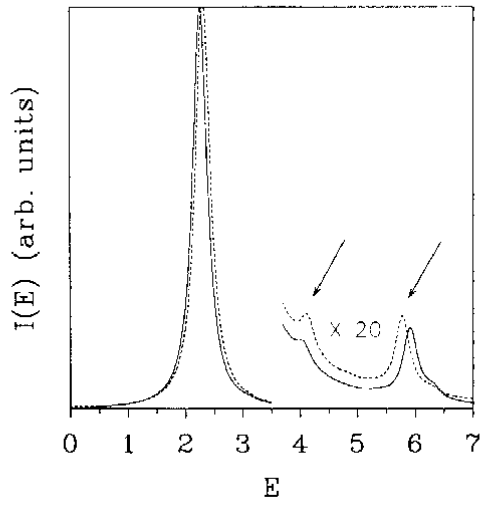

Fig. 1. Absorption spectra for a Fibonacci lattice with $N = F_{12} = 233$ active centers and on-site energies $V_A = 4.0$ and $V_B = 4.8$. The solid line indicates the numerical result and the dashed line the analytical approach.

Therefore, the spectrum consists of a main Lorentzian line centered at $E_0^{(AB)} = cV_B + (1-c)V_A - 2J = 2.30$, in agreement with the virtual crystal approximation, and several satellite lines at $E_k^{(AB)}$. The most remarkable fact of expression (9), however, is that it relates the finer details of the absorption spectrum, an experimentally measurable magnitude, with the Fourier transform of the lattice describing the topological long-range ordering of the optical centers. To demonstrate this point, we recall that unperturbed eigenvectors are orthogonal. Thus

$$\langle 0|\mathscr{H}_{AB}|k\rangle = \left\langle 0\left|\sum_n (V_n - V_A)a_n^\dagger a_n\right|k\right\rangle = \frac{1}{N}\sum_n V_n \exp(2\pi i kn/N), \quad k \neq 0, \tag{11}$$

which is nothing but the aforementioned Fourier transform. A comparison of the perturbative prediction (9) with the numerical results is given in Fig. 1, where an excellent agreement is achieved in the weak-perturbation limit we have considered. In particular, our analytical approach predicts the existence of two satellite lines at $E^{(1)} = 5.78$ and $E^{(2)} = 4.13$.

In order to get a deeper insight into the problem, we relate our results with those reported in the

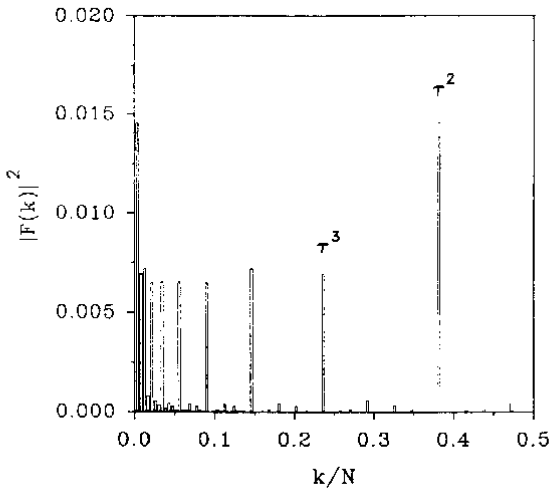

Fig. 2. Plot of $|F(k)|^2$ as a function of the ratio k/N for Fibonacci lattices, showing the occurrence of well-defined Bragg peaks, labelled according to successive powers of τ.

various works dealing with the Fourier transform of the Fibonacci sequence, some of them in connection with X-ray diffraction in aperiodic semiconductor superlattices [13,14]. The Fibonacci lattice is known to exhibit a Fourier spectrum displaying well-defined Bragg peaks. The Fourier intensity $|\langle 0|\mathscr{H}_{AB}|k\rangle|^2$ consists of a series of peaks located at values of the momentum $2\pi\ k/N$ of the form τ^p, where p is an arbitrary integer. Each peak of the Fourier intensity leads to a large contribution to the sum (9) and, consequently, to a well-defined satellite line in the absorption spectrum.

Fig. 2 shows $|F(k)|^2$ as a function of the ratio k/N evaluated from expression (10), the results being independent of the system size. A sequence of Bragg peaks, arranged according to successive powers of τ, are clearly observed in this plot. The stronger one, which is responsible for the highest-energy satellite line centered at $E^{(1)} = 5.78$, is located at $k_p/N \simeq 0.38 \simeq \tau^2$ $(p = 2)$. Therefore the mode is located close to the top of the excitonic band $(k/N = 0.5)$. On decreasing the momentum, the next Bragg peak is located at $k_p/N \simeq 0.23 \simeq \tau^3$ $(p = 3)$, leading to an energy value 4.13, in perfect agreement with the energy of the second satellite peak in the high-energy region of the spectrum observed in Fig. 1. The analytical treatment predicts the existence of other satellite lines with smaller energy, but they are hidden by the main absorption line.

Our results are suitable for a direct physical interpretation. Each satellite line of high energy is caused by the coupling of two modes, namely the lowest-lying and k_p, through the topology of the quasiperiodic lattice. Notice that a different arrangement of the centers would lead to a completely different Fourier intensity $|\langle 0|\mathscr{H}_{AB}|k\rangle|^2$. Thus, the exciton acts as a probe of the long-range order of the quasiperiodic lattice. This is one of the main results of the present work since it provides us with a useful method to be applied in experimental situations.

5. Conclusions

In summary, we have studied numerically the absorption spectra corresponding to the Frenkel-exciton Hamiltonian on self-similar quasiperiodic Fibonacci lattices. Besides the main line, which is shifted with respect to that of the pure lattice, we found several satellite lines in the high-energy region of the absorption spectra. We have also developed an analytical method which successfully explains not only the shift of the main line and the position of the satellite lines but also their shape. Our analysis clearly indicates that each satellite line is directly related to a particular Bragg peak of the Fourier transform of the underlying lattice. We have shown that each satellite line comes from the coupling between the lowest-lying mode and a particular mode lying close to the top of the excitonic band. This relationship surely should facilitate future experimental work on optical properties of molecular systems with long-range order.

Acknowledgment

The author thanks E. Maciá, A. Sánchez and V. Malyshev for helpful comments. This work is supported by CICYT through project MAT95-0325.

References

[1] S.-R. Eric and S. Das Sarma, Phys. Rev. B 37 (1988) 4007.
[2] A.A. Yamaguchi, T. Saiki, T. Tada, T. Ninoyima, K. Misawa and T. Kobayashi, Solid State Commun. 85 (1993) 223.

[3] D. Tuet, M. Potemski, Y.Y. Wang, J.C. Maan, L. Tapfer and K. Ploog, Phys. Rev. Lett. 66 (1991) 2128.
[4] D. Munzar, L. Bočáek, J. Humlíček and J. Ploog, J. Phys. Condens. Matter 6 (1994) 4107.
[5] E. Maciá and F. Domínguez-Adame, Phys. Rev. B 50 (1994) 16856.
[6] F. Domínguez-Adame, E. Maciá and A. Sánchez, Phys. Rev. B 51 (1995) 878.
[7] N. Niu and F. Nori, Phys. Rev. Lett. 57 (1986) 2057; Phys. Rev. B 42 (1990) 10329.
[8] Y. Liu and W. Sritrakool, Phys. Rev. B 43 (1991) 1110.
[9] D.L. Huber and W.Y. Ching, Phys. Rev. B 39 (1989) 8652.
[10] W.H. Press, S.A. Teukolsky, W.T. Vetterling and B.P. Flannery, Numerical recipes in C, 2nd Ed. (Cambridge Univ. Press, Cambridge, 1992).
[11] F. Domínguez-Adame, E. Maciá and A. Sánchez, Phys. Rev. B 50 (1994) 6453.
[12] F. Domínguez-Adame, Phys. Rev. B 51 (1995) 12801.
[13] R. Merlin, IEEE J. Quantum Electron. 24 (1988) 1791, and references therein.
[14] C. Godrèche and J.M. Luck, J. Phys. A 23 (1990) 3769.